Applied Energy 138 (2015) 533–545

Contents lists available at ScienceDirect

Applied Energy

journal homepage: www.elsevier.com/locate/apenergy

Experimental assessment of the energy performance of a hybrid desiccant cooling system and comparison with other air-conditioning technologies

Giovanni Angrisani *, Carlo Roselli, Maurizio Sasso

DING, Department of Engineering, Università degli Studi del Sannio, Benevento, Italy

HIGHLIGHTS

- Performance of a desiccant cooling system are investigated through energy analysis.
- Both the overall hybrid system and the desiccant rotor alone are analyzed.
- The effect of five operating variables on performance is analyzed.
- Suitable working range for each operating variable is defined.
- Energy and emissions comparisons with other air-cooling technologies are performed.

ARTICLE INFO

Article history:
Received 17 April 2014
Received in revised form 2 September 2014
Accepted 24 October 2014
Available online 21 November 2014

Keywords:
Desiccant cooling
Air handling unit
Microcogenerator
Performance parameters
Energy analysis
Air-conditioning

ABSTRACT

Desiccant-based air handling units (AHU) can allow significant energy saving and emissions reductions with respect to conventional air-conditioning systems. In this work, experimental tests are used to investigate a hybrid desiccant cooling system (DCS) with desiccant wheel (DW), interacting with a small scale cogenerator.

Several new contributions are introduced by this study, such as the high number of operating conditions analyzed and of performance parameters used, the definition of a new COP and a comparison of the DCS with other air-conditioning options.

The performance were analyzed varying five operating conditions: regeneration temperature, rotational speed, volume air flow rates, outdoor air temperature and humidity ratio. Several performance parameters, based on electric, thermal and primary energy, are investigated.

Thermal performance of both the overall hybrid DCS and the DW reduce when regeneration temperature or flow rate increase, while electric and primary energy based parameters rise. Optimal operation is instead found for a narrow range of rotational speed.

The hybrid DCS with microcogenerator is compared with other thermal or electrical air-conditioning technologies. The investigated DCS performs better or at least equal than the other thermally-activated systems, while the result of the comparison with the conventional electric unit depends on the outdoor air conditions.

1. Introduction

Desiccant cooling systems (DCS), using either solid [1–3] or liquid [4,5] desiccant materials, are an interesting alternative to conventional systems with electrically-driven vapor compression cooling units, [6–9]. The main energy requirement is low temperature heat, which can be supplied by thermal wastes [10] or solar thermal energy [7,11], typically integrated with an auxiliary fossil-fuelled system. In a hybrid DCS an electric chiller contributes to balance the sensible load.

Desiccant dehumidification until now has been mostly used in niche markets (electronics, food and arms storage, pharmaceutical industry, hospitals). During last years, thanks to its benefits, this technology is also spreading in applications with high latent loads, such as supermarkets, ice arenas, restaurants, theatres, schools and museums, as well as in residential and tertiary sectors; nevertheless, this technique is still rarely implemented in Europe, due to several obstacles, such as high investment costs, low familiarity, lack of knowledge about performances and cost/benefit ratio.

* Corresponding author. Tel.: +39 0824 305576; fax: +39 0824 325246.
E-mail address: giovanni.angrisani@unisannio.it (G. Angrisani).

http://dx.doi.org/10.1016/j.apenergy.2014.10.065
0306-2619/

Nomenclature

COP	Coefficient of Performance, –
E	energy, MWh
F_{bp}	by-pass factor, –
h	enthalpy, kJ/kg
$\dot{m}$	mass flow rate, kg/s
N	rotational speed, rev/h
NE	net energy, MWh
P	power, kW
PE	primary energy, MWh
PER	primary energy ratio, –
t	temperature, °C
$\dot{V}$	volumetric air flow rate, m^3/h

Acronyms

ACH	absorption chiller
ADCH	adsorption chiller
AHU	air handling unit
CHP	Combined Heat and Power
DCS	desiccant cooling system
DW	desiccant wheel
HP	heat pump
HVAC	eating ventilation and air-conditioning
LDAC	liquid desiccant air-conditioning
MCHP	Micro Combined Heat and Power
SP	separate production
VCS	vapor compression system

Greek symbols

$\Delta CO_{2,eq}$	avoided equivalent CO_2 emissions, –
ε_{hc}	effectiveness of the heating coil, –
η	efficiency, –
μ	specific emission factor, $g_{CO2,eq}/kWh$
ω	air humidity ratio, g/kg
τ	time, s

Subscripts

conv	conventional
Cool	cooling
$CO_{2,eq}$	equivalent carbon dioxide
El	electric
Fuel	fuel primary energy
NG	natural gas
out	outdoor
PE	primary energy
proc	process air
ref	reference system
reg	regeneration air
s	saturated condition
sup	supply air
sorpt	sorptive
Th	thermal
tot	total

Superscripts

ACH	absorption chiller
ADCH	adsorption chiller
AHU	air handling unit
aux	auxiliaries
comp	chiller compressor
DCS	desiccant cooling system
fan	condenser fan
GB	gas boiler
MCHP	micro combined heat and power
ph	post heating
SP	separate production
VCS	vapor compression system

Energy performance assessment of DCS is a non-trivial task; several parameters have been used in literature to evaluate the energy performance of DCS, assessing the effect of several operating parameters. Exergy analysis of both solid and liquid DCS has also been performed, [12,13].

Actually, every DCS is very peculiar, and no standards exist about testing or performance coefficients definition. However, a reasonable and meaningful comparison between the different installations can be effectively carried out if several performance parameters are contemporary used, related to the overall system, to the air handling unit (AHU) only or to a part of it (such as the desiccant rotor). These performance parameters should allow to overcome the peculiarities of each system, taking into account the specific layout of the AHU, the energy requirements of the system (electricity, heat, primary energy) and the energy conversion devices used (based on either fossil fuels or renewables). Such performance parameters can also be used to compare a DCS with other air-conditioning technologies, in order to assess the more suitable system for a given application and climatic condition.

The COP is the commonly used parameter to characterize the performance of cooling equipment; it is the ratio between the useful cooling effect to the required energy input. For DCS, different COPs can be defined: the thermal COP considers heat input for regeneration, while the electric COP considers electric energy input, for auxiliaries and chiller, in the case of hybrid DCS. Furthermore, the COP can take into account the overall cooling effect, or only the amount which is not covered by the cooling coils, if any; in this case, it is usually defined as sorptive COP.

Henning et al. [2] presented the design of an advanced desiccant air handling unit using a high efficient combination of a vapor compression chiller and a desiccant wheel (DW). Electricity for the chiller was supplied by a CHP (Combined Heat and Power) system and thermal energy to regenerate the desiccant material was the recovered heat from the CHP. In order to compare the performance of the different layouts, several performance figures were defined. The sorptive COP varied in the range 0.41–1.34 and the electricity saving with respect to a reference system varied in the range 25.6–34.3%, depending on the system configuration.

Panaras et al. [14] identified the main design parameters of a solid desiccant air-conditioning systems, and investigated their effect on the performance of the systems. The air flow rate, the regeneration temperature, the operation cycle and the subsystems level of performance constituted the design parameters. The thermal COP reduced with both regeneration temperature and air flow rate, and it was higher for the ventilation cycle (maximum value of about 0.5) than the recirculation one (maximum value of about 0.4). The COP raised to 0.85 for the ventilation cycle in the case of high level performance of the desiccant rotor.

Heidarinejad and Pasdarshahri [15] developed a desiccant cooling model and applied it to different operating modes of the system. The effects of the regeneration temperature and rotational speed of the desiccant wheel on thermal COP were investigated. The COP reduced when regeneration temperature increased and when rotational speed decreased. Maximum values in the range 0.25–0.29 were found for the minimum regeneration temperature investigated (60 °C).

Heidarinejad and Pasdarshahri [16] analyzed a DCS applied to two operating cycles: one using return air from the building for regeneration, one using outdoor air. A mathematical model of desiccant component based on transient and coupled heat and mass transfer was derived and validated using experimental measurements. Thermal COP was chosen as performance parameter, with cooling effect defined as the enthalpy difference between supply and indoor conditions. The COP increased up to about 0.34, when either outdoor temperature and humidity increased.

Nóbrega and Brum [17] presented a design methodology for DCS, which can be easily carried out graphically on a psychrometric chart. A standard layout of the DCS was considered. The effect of the regeneration temperature and of the effectiveness of the heat wheel was investigated. The thermal COP achieved a maximum value of about 0.4, with regeneration temperature of 110 °C and effectiveness of the heat wheel equal to 0.9.

Jalalzadeh-Azar et al. [18] evaluated the performance of a DCS, in which thermal energy for regeneration was provided by heat recovery from a gas-fired reciprocating internal combustion engine. Electrical and thermal COP were investigated as a function of outdoor ambient temperature, with two humidity ratio values (low and high humidity). Both COP increased with ambient temperature and humidity; moreover, the DCS operated with an electrical COP of about 5.3, which is more efficient than typical conventional systems.

Hürdoğan et al. [19] designed and tested a novel desiccant based air-conditioning system to improve indoor air quality and reduce energy consumption. The COP of the system was defined as the ratio between the cooling capacity and total energy input to the system, which is the sum of heat consumption for regeneration and electricity for auxiliaries and for the vapor compression refrigeration cycle. The COP varied from 0.4 to 4 during the day, with a mean value of 1.35.

Ali Mandegari and Pahlavanzadeh [20] experimentally investigated the operation of a DCS. Different climates were investigated by changing the temperature and humidity of inlet air. Thermal and electrical COP of the DCS were evaluated, as well as an overall COP, which considered the total energy consumption. As a reference situation, a vapor compression system (VCS) was examined. Overall COP of DCS in comparison with VCS decreased about 36% and 28% in hot–dry and hot–humid climates, respectively, due to the high thermal energy consumption in DCS. In contrast its electric COP increased, therefore by using DCS some electrical energy would be saved.

Çarpinlioglu and Yildirim [21] experimentally analyzed an open cycle DCS operating with ventilation mode. The rotational speeds of rotary regenerator and desiccant wheel, air mass flow rate in process and regeneration lines, and the regeneration temperature were defined as operation parameters. Thermal COP increased with air mass flow rate and it decreased with regeneration temperature and rotational speed of DW, while the rotational speed of the rotary regenerator did not cause a significant influence on the magnitudes of COP.

Eicker et al. [22] conducted experimental investigations on several commercially available and newly fabricated rotors. Four figures of merit were described, such as the Regeneration Specific Heat Input, which is the regeneration thermal power supplied to the device in relation to the dehumidification capacity flux. It was found for example that the optimal rotation speed is lower for lithium chloride or compound rotors than for silica gel rotors.

Tu et al. [23] analyzed the performance of a heat pump-driven two-stage desiccant wheel system, with three evaporators and three condensers located in the process and regeneration air flow, respectively. The effects on system performance of several operating conditions, such as the rotation speed of the wheel and the inlet parameters of the processed air were investigated. The COP was defined as the ratio between the cooling capacity of the process air to the power input of the compressor. For example when the supplied air humidity ratio is 10 g/kg, COP is 5.5 under Beijing summer condition.

The reviewed studies are not comprehensive, in terms of parameters used and operating conditions investigated. Therefore, one of the novelties of this work is that experimental tests are used to investigate a hybrid DCS with DW, considering the performance of both the overall system and the desiccant rotor alone, varying the effect of five independent variables: regeneration temperature (t_{reg}), rotational speed (N), ratio between flow rates of regeneration and process air ($\dot{V}_{reg}/\dot{V}_{proc}$), outdoor air temperature (t_{out}) and humidity ratio (ω_{out}). The variations of t_{reg}, N and air flow rates are the typically adopted control strategies of DCS, [24–26].

A further new contribution is that several parameters, based on electric, thermal and primary energy, are defined to allow a more comprehensive performance assessment and to locate the suitable operating range for each variable. A completely new performance parameter is also introduced with respect to existing literature.

Furthermore, no one of the reviewed papers performs an accurate comparison of DCS with several other technologies for given operating conditions; therefore, another new aspect of this paper is that the hybrid DCS is compared with other electrically and thermally-activated air-conditioning options: DCS with separate "production" systems (with and without integrated heat pump), liquid desiccant cooling as well as conventional AHU interacting with electric vapor compression, absorption or adsorption chiller.

2. Test facility

At "Università degli Studi del Sannio", in Benevento (Southern Italy), a desiccant-based AHU coupled to an electric chiller and a natural gas-fired boiler (Fig. 1), is currently experimentally analyzed. The HVAC (Heating, Ventilation and Air Conditioning) system is based on the dehumidification of outdoor air by a desiccant wheel and its subsequent cooling by an electric chiller. In Table 1 the symbol, measuring range and accuracy of the installed sensors is shown.

Nominal characteristics of the devices are the following:

- MCHP (Micro Combined Heat and Power): unit based on a natural gas fuelled internal combustion engine, nominal thermal power output 11.7 kW, gross electric power output 6 kW, primary fuel requirement 20.8 kW;
- electric air-cooled water chiller based on VCS: cooling capacity 8.50 kW, COP^{VCS} 3.00;
- boiler: fuelled by natural gas, 24.1 kW thermal power, 90.2% nominal efficiency. The boiler can be used to integrate the thermal power available from the MCHP;
- desiccant wheel: filled with silica-gel, a desiccant material that can be effectively regenerated at temperatures as low as 60–70 °C. The DW has a weight of 50 kg and its dimensions are 700 mm × 200 mm (diameter × thickness). Due to the metallic frame of the wheel cassette, the diameter of the active portion of the wheel is 600 mm. Sixty percent of the rotor area is crossed by the process air, while the remaining 40% by the regeneration air. The nominal rotational speed of the DW is 12 rev/h.

As regards the AHU, there are three outdoor air streams, each one with a nominal volumetric flow rate of 800 m^3/h (Figs. 1 and 2). The air flows are entirely drawn from the outdoor (state 1 in Fig. 1, common to the three airflows), therefore no recirculation is carried out:

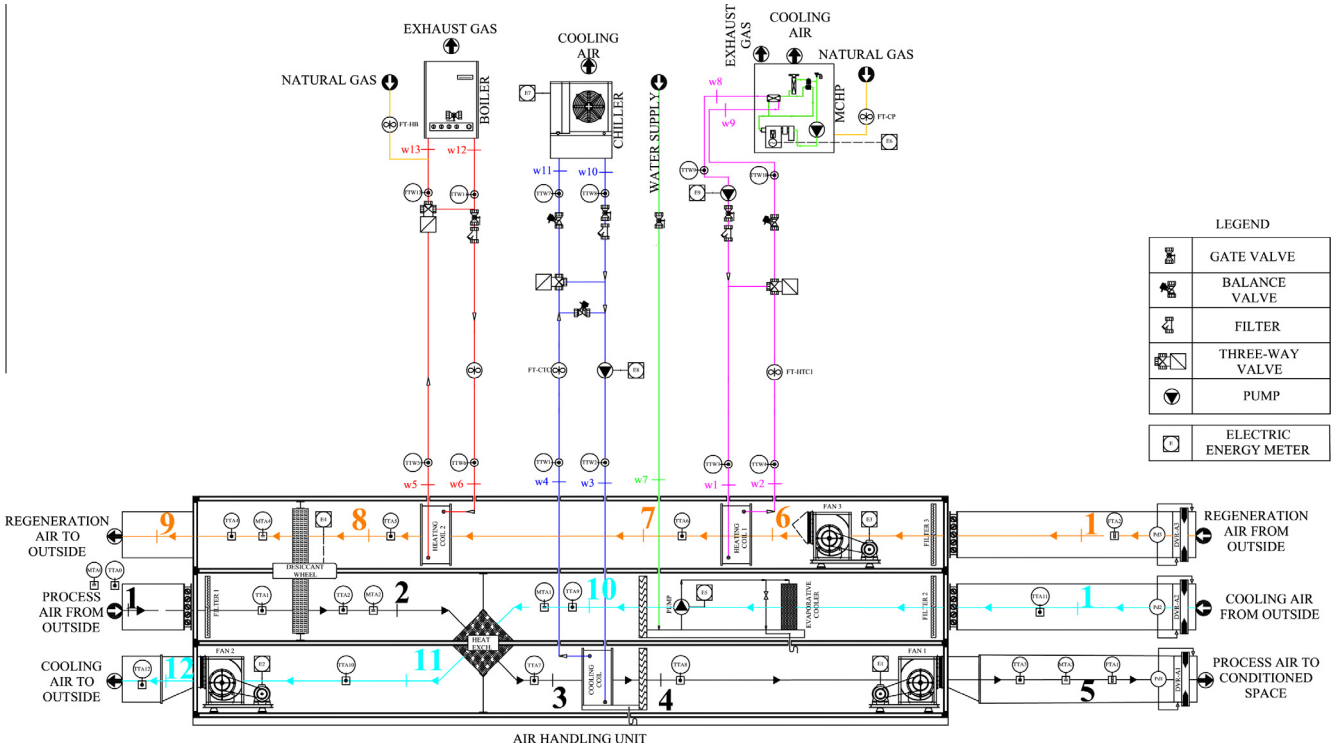

Fig. 1. The layout of the hybrid DCS.

Table 1
Symbol, measuring range and accuracy of the installed sensors.

Symbol	Measured parameter	Measuring range	Accuracy
TTA	Air temperature	−50/+50 °C	±0.5 °C
TA	Air temperature	−10/+90 °C	±0.15 °C
MTA	Ambient relative humidity	0–99%	±2% RH (5–90% RH) ±2.5% RH (0–5% and 90–100% RH)
FTA	Air velocity	0–10 m/s	±0.2 m/s + 3% of measured value
TTW	Water temperature	−10/+120 °C	±1.4 °C
	Volumetric flow rate	2–60 L/min	±2% of full scale
	Mass flow rate	0–2.5 Nm^3/h	±0.2% of full scale

- process air, dehumidified by the desiccant wheel (1–2), pre-cooled by the cooling air stream in an air-to-air cross flow heat exchanger (2–3), finally cooled to the supply temperature by a cooling coil interacting with the chiller (3–4) and supplied to the conditioned space by the related fan (4–5); state 4 is not shown in Fig. 2 for major clarity, as it is very close to state 5;
- regeneration air, drawn from outside (1–6), heated by the heating coil interacting with the MCHP (6–7) and/or the boiler (7–8); it is used to regenerate the desiccant wheel (8–9); state 6 is not shown in Fig. 2 for major clarity, as it is very close to state 1;
- cooling air, cooled by a humidifier (1–10), then used to pre-cool the process air exiting the desiccant wheel (10–11), and finally exhausted to the outside (11–12); state 12 is not shown in Fig. 2 for major clarity, as it is very close to state 11.

The effectiveness of the AHU components was experimentally determined in [27].Considering $t_1 = 32$ °C, $\omega_1 = 15$ g/kg, $t_5 = 13$ °C, $\omega_5 = 7$ g/kg, volumetric flow rate of process air $\dot{V}_{proc} = 800$ m^3/h, the nominal cooling capacity of the hybrid DCS is 10 kW.

In Fig. 2, the processes of the conventional AHU are also shown. They will be explained in Section 4.2.3.

The circulation pumps of the MCHP, the boiler and the chiller have an electric requirement of 150 W each; the humidifier pump requires about 30 W; the DW motor requires 10 W; the four speeds process, regeneration and cooling air fans require 320 W each.

The main energy flows of the system during summer operation are shown in Fig. 3. Specific superscripts, referring to energy conversion devices involved in an energy flow, have been used. When two superscripts are present, the former refers to the output device, the latter to the input one. Subscripts refer instead to energy vectors.

3. Methodology

To evaluate the performance of the DCS (refer to Fig. 1 for state points of process and regeneration air) as a function of regeneration air temperature (t_{reg} equal to t_8, temperature of state 8 in Fig. 1), rotational speed (N), ratio between regeneration and process air volumetric flow rate ($\dot{V}_{reg}/\dot{V}_{proc}$), outdoor air temperature (t_{out} equal to t_1, temperature of state 1 in Fig. 1) and humidity ratio (ω_{out} equal to ω_1, humidity ratio of state 1 in Fig. 1), several coefficients of performance have been analyzed.

The total net cooling energy, NE^{DCS}_{Cool}, is defined as the time integral of the enthalpy difference between ambient air and supply air multiplied by the process air mass flow rate:

$$NE^{DCS}_{Cool} = \int \dot{m}_{proc} \cdot (h_1 - h_5) d\tau \quad (1)$$

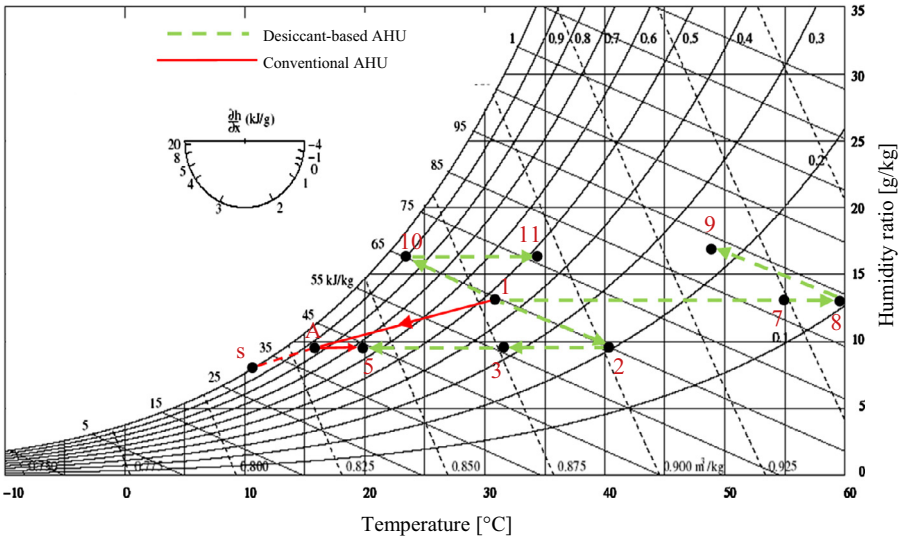

Fig. 2. The processes relative to desiccant-based and conventional AHU.

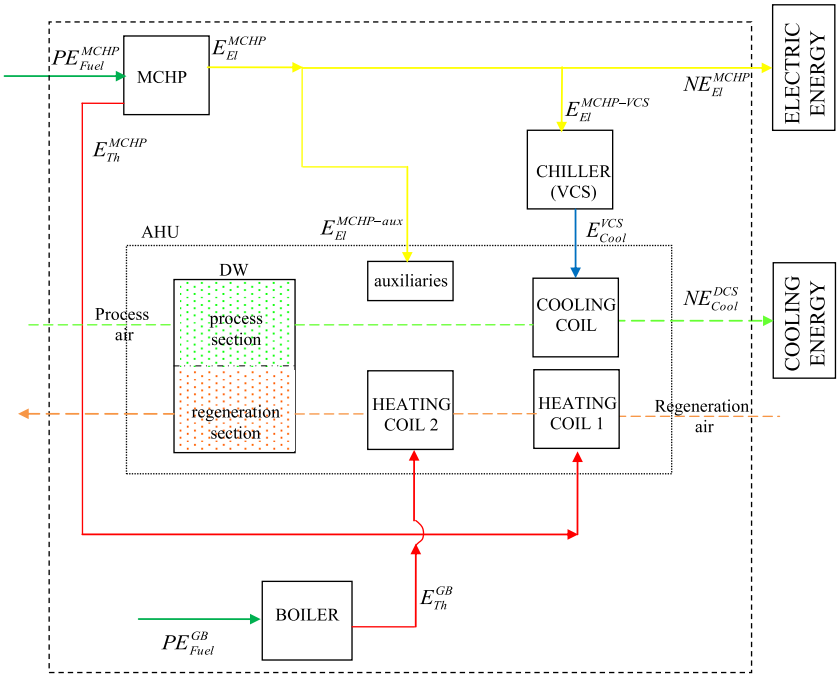

Fig. 3. Main energy flows of the system during summer operation.

The thermal Coefficient of Performance of the desiccant cycle is then determined by [28]:

$$COP_{Th} = \frac{NE_{Cool}^{DCS}}{\int \dot{m}_{reg}(h_8 - h_1)d\tau} \quad (2)$$

where the denominator represents thermal energy required for DW regeneration.

The electrical COP of the desiccant cycle is determined by:

$$COP_{El} = \frac{NE_{Cool}^{DCS}}{E_{El,tot}} \quad (3)$$

where $E_{El,tot}$ is the overall electricity consumption of AHU auxiliaries (fans and pumps, $E_{El}^{MCHP-aux}$) and of the electric chiller, $E_{El}^{MCHP-VCS}$.

The *PER* (Primary Energy Ratio) is defined as the ratio between the useful outputs (cooling and electric energy) and total primary energy input of MCHP and boiler:

$$PER = \frac{NE_{Cool}^{DCS} + NE_{El}^{MCHP}}{PE_{Fuel}^{MCHP} + PE_{Fuel}^{GB}} \quad (4)$$

During the tests, the MCHP worked at full thermal and electric load; when electric power output is higher than requirements of auxiliaries and chiller, the electricity surplus (NE_{El}^{MCHP}) is used to activate electric appliances of the user (lights, computers, etc.).

Eqs. (1)–(4) refer to the overall hybrid DCS, while the following ones are used to assess the performance of its sorptive part only, i.e. the desiccant rotor.

The conventional net cooling energy, $NE^{DCS}_{Cool,conv}$, denotes the cooling effect supplied by the cooling coil, using chilled water supplied by the compression chiller, [2]:

$$NE^{DCS}_{Cool,conv} = \int \dot{m}_{proc} \cdot (h_3 - h_4) d\tau \quad (5)$$

The sorptive net cooling energy, $NE^{DCS}_{Cool,sorpt}$, defines the amount of the total cooling which is not covered by the cooling coil:

$$NE^{DCS}_{Cool,sorpt} = NE^{DCS}_{Cool} - NE^{DCS}_{Cool,conv} = \int \dot{m}_{proc} \cdot [(h_1 - h_5) - (h_3 - h_4)] d\tau \quad (6)$$

Since the dehumidification process is nearly isenthalpic ($h_1 \cong h_2$), [6], and $h_4 \cong h_5$, Eq. (6) can be rewritten as:

$$NE^{DCS}_{Cool,sorpt} \cong \int \dot{m}_{proc} \cdot (h_2 - h_3) d\tau \quad (7)$$

Therefore, the sorptive net cooling energy is almost fully provided by the cross flow heat exchanger in the investigated system.

The sorptive thermal COP is defined as the ratio between the sorptive cooling and the required thermal energy for regeneration of the desiccant:

$$COP_{Th,sorpt} = \frac{NE^{DCS}_{Cool,sorpt}}{\int \dot{m}_{reg}(h_8 - h_1) d\tau} \quad (8)$$

The ratio between $COP_{Th,sorpt}$ and COP_{Th} (as well as the ratio between $NE^{DCS}_{Cool,sorpt}$ and NE^{DCS}_{Cool}) represents the amount of the total cooling effect that is not provided by the cooling coil interacting with the conventional chiller.

The sorptive electric COP is defined as the ratio between the sorptive cooling and the electricity consumption of the sorptive part of the hybrid DCS:

$$COP_{El,sorpt} = \frac{NE^{DCS}_{Cool,sorpt}}{E^{DCS}_{El}} \quad (9)$$

E^{DCS}_{El} is the electricity consumption of the circulation pumps (MCHP and boiler), of the humidifier pump and of the 3 fans, excluding the electricity consumption of the conventional VCS (the chiller and the related pump). To the authors' knowledge, $COP_{El,sorpt}$ was never used in scientific literature, and it can provide useful information about how the auxiliaries of the DCS should be managed to maximize the sorptive cooling effect.

The comparisons between the hybrid DCS with other electrically and thermally-activated air-conditioning technologies have been performed, considering equal useful outputs of the compared systems, on the basis of both energy and emissions analysis; the former have been based on the same performance factor previously defined, while the latter focuses on the possibility to reduce the equivalent CO_2 emissions with respect to the compared system; therefore, the assessment index is the equivalent CO_2 avoided emission, $\Delta CO_{2,eq}$ [29].

In this paper, the following values are used, given the Italian energy context:

- energy performance factor of Italian reference system for electricity supply (electric grid), including transmission and distribution losses (ratio of electric energy output to primary energy input), $\eta_{El,ref} = 42.0\%$, [10];
- energy performance factor of reference system for thermal energy supply (natural gas boiler), $\eta_{Th,ref} = 82.8\%$, average value derived from experimental tests, [10];
- equivalent carbon dioxide specific emission factors of Italian reference system for electricity supply (ratio of equivalent CO_2 emissions to electric energy output), $\mu_{El,ref} = 573\ g_{CO2,eq}/kWh_{EI}$, [10];
- equivalent carbon dioxide emission factor of natural gas (ratio of equivalent CO_2 emissions to primary energy input), $\mu_{NG} = 207\ g_{CO2,eq}/kWh_{PE}$.

4. Results

4.1. Performance of the hybrid DCS with MCHP

In this section, the performance of the overall hybrid DCS (COP_{Th}, COP_{El} and PER) as well as those of the sorptive part only ($COP_{Th,sorpt}$ and $COP_{El,sorpt}$) are shown as a function of five independent operating variables: regeneration temperature and rotational velocity of the DW, ratio between regeneration and process air flow rates, outdoor air temperature and humidity ratio. In the caption of each figure, the values of the independent operating conditions being constant during the test, as well as the supply temperature (t_{sup} equal to t_5, temperature of state 5 in Fig. 1) and humidity ratio (ω_{sup} equal to ω_5, humidity ratio of state 5 in Fig. 1), the supply water temperature from the chiller (t_{w10} in Fig. 1) and its average COP^{VCS} are reported. Generally, volumetric flow rates are different from the nominal values. Each experimental point represents the average of a test at stationary conditions with a duration of 30 min and a measurement frequency of 1 Hz.

In Fig. 4, the performance parameters for the overall DCS (Fig. 4a) and for the desiccant rotor (Fig. 4b), as a function of regeneration temperature, are shown. As process and regeneration air flow rates are constant, the increase of t_{reg} determines a strong reduction of COP_{Th}, from 2.1 to 0.7 when regeneration temperature increases from 40 to 70 °C. The adoption of low temperatures, however, determines low moisture removal capacity and dehumidification effectiveness of the DW, [30].

These results are also confirmed by Ge et al. [31], who simulated a solar driven two-stage rotary desiccant cooling system to provide cooling for one floor in a commercial office building in two cities with different climates, Berlin and Shanghai. A COP_{Th} of 0.9 and 1.28 was obtained, with t_{reg} equal to 55 °C and 85 °C, respectively. Furthermore, Wang et al. [32] stated that under ARI (American Air conditioning and Refrigeration Institute) summer conditions ($t_{out} = 35$ °C, $\omega_{out} = 14.3$ g/kg, velocity of air 0.8 m/s, temperature of indoor air 26.7 °C, humidity ratio of indoor air 11.1 g/kg) the two-stage rotary desiccant cooling system at $t_{reg} = 60$ °C can achieve a COP_{Th} equal to 1.16. Ge et al. [33] concluded that the thermal COP of the two-stage DW kept over 1 if regeneration temperature is not higher than 70 °C. These studies corroborate the results of the present investigation, considering that a single-stage DW is here analyzed.

On the contrary, COP_{El} is influenced by two counteracting effects when t_{reg} rises: on one side the cooling load on the chiller increases as well as the required electric power, due to the increased heating of process air, [6]; on the other side, the cooling effect increases due to the rise of the humidity ratio reduction on process air, [6]. The latter effect slightly prevails and determines the increase of both the performance factors based on electric and primary energy.

As regards the performance of the desiccant rotor, $COP_{Th,sorpt}$ reduces with t_{reg}, similarly to COP_{Th}. The ratio between $COP_{Th,sorpt}$ and COP_{Th} is nearly constant at slightly less than 0.3, therefore more than 70% of the total cooling energy is provided by the cooling coil. Finally, $COP_{El,sorpt}$ initially improves due to the increase of the sorptive useful cooling effect, then it saturates at a constant value: in fact, to reach regeneration temperatures higher than 65 °C, the boiler and the related circulation pump has to be switched on, thus raising the electricity consumption of the DCS.

In Fig. 5, the performance as a function of rotational speed are shown. All the parameters related to the overall system (Fig. 5a) shows a peak value for a certain optimum velocity, in the range

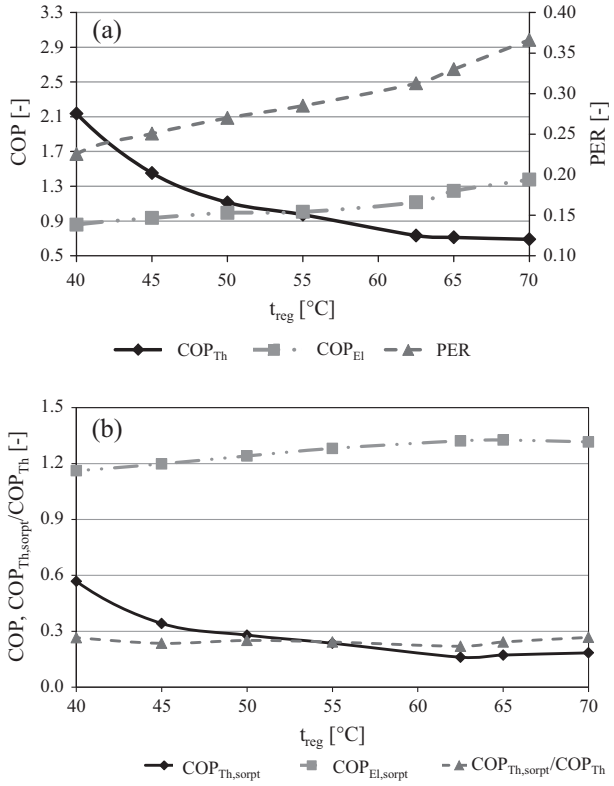

Fig. 4. Performance parameters as a function of regeneration temperature – t_{out} = 32.7 °C, ω_{out} = 13.0 g/kg, N = 12 rev/h, $\dot{V}_{proc}$ = 579 m³/h, $\dot{V}_{reg}$ = 734 m³/h, t_{sup} = 16.1 °C, ω_{sup} = 8.88 g/kg, t_{w10} = 10.8 °C, COP^{VCS} = 2.41.

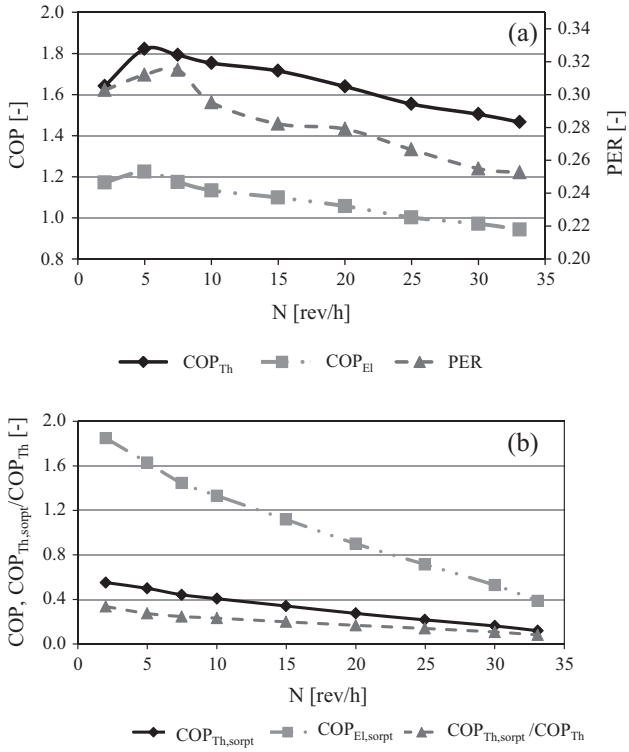

Fig. 5. Performance parameters as a function of rotational speed – t_{out} = 34.3 °C, ω_{out} = 11.1 g/kg, t_{reg} = 55.0 °C, $\dot{V}_{proc}$ = 579 m³/h, $\dot{V}_{reg}$ = 477 m³/h, t_{sup} = 17.1 °C, ω_{sup} = 6.94 g/kg, t_{w10} = 4.72 °C, COP^{VCS} = 2.11.

2–7.5 rev/h, because in this range the dehumidification performance of the DW are maximum, [26].

As regards $COP_{Th,sorpt}$ and $COP_{El,sorpt}$, both the regeneration thermal power and the electricity consumption of the DCS are almost not affected by rotational speed; however, the increase of N determines an augmented heating of process air through the DW, [26]. Therefore, as the total cooling effect is constant, the sensible load on the electric chiller increases while $NE^{DCS}_{Cool,sorpt}$ reduces, as well as the sorptive thermal and electric COPs. The $COP_{Th,sorpt}/COP_{Th}$ ratio reduces from about 0.35 to less than 0.10: the increase of the rotational speed determines a rise in the share of total cooling effect provided by the chiller through the cooling coil, due to the augmented sensible cooling load.

In Fig. 6, the influence of the parameter $\dot{V}_{reg}/\dot{V}_{proc}$, which is the ratio between the regeneration to the process air flow rates, is analyzed: during the performed tests, the process air flow rate was kept constant, while varying the regeneration air flow rate only. The increase of the latter flow rate determines an increase of the regeneration thermal power, therefore both COP_{Th} (Fig. 6a) and $COP_{Th,sorpt}$ (Fig. 6b) reduce.

COP_{El} is affected by two counteracting effects: when $\dot{V}_{reg}$ increase, there is an improvement of the moisture removal capacity of the DW and of the related cooling effect, [30]; on the other side, the electric power required by regeneration air fan slightly rises; the former effect prevails, thus electric COP improves with regeneration air flow rate. Similarly, the *PER* increases with $\dot{V}_{reg}$, due to the augmentation of the useful cooling effect.

$COP_{El,sorpt}$ shows a maximum value at $\dot{V}_{reg}/\dot{V}_{proc}$ = 0.6 (Fig. 6b): it initially improves, due to the enhancement of $NE^{DCS}_{Cool,sorpt}$ with $\dot{V}_{reg}$; then it reduces due to the increase of the electricity consumption of the regeneration fan.

The contribution of the sorptive system to the overall cooling effect is nearly constant at about 20%.

Fig. 7 shows the performance of the DCS and of the DW as a function of outdoor air temperature. The increase of $t_{out} = t_1$ determines the rise of both NE^{DCS}_{Cool} and $NE^{DCS}_{Cool,sorpt}$ and, above all, a reduction of regeneration thermal power required, as $t_{reg} = t_8$ is constant, [6,30]; therefore COP_{Th} and $COP_{Th,sorpt}$ increase. As regards COP_{El}, the slight increase of NE^{DCS}_{Cool} is offset by the rise in the electric power required by the chiller; therefore the electric COP is almost not affected by outdoor air temperature (Fig. 7a), even if slightly lower values can be found for very low and very high values of t_{out}. A similar trend can be observed for the *PER*.

Moreover, as $NE^{DCS}_{Cool,sorpt}$ increases with t_1 while E^{DCS}_{El} remains constant, $COP_{El,sorpt}$ increases with outdoor air temperature. Finally, the $COP_{Th,sorpt}/COP_{Th}$ ratio increases with t_{out}, in the range 0.16–0.25.

The effect of outdoor air humidity ratio on the system is shown in Fig. 8. The performance of the overall DCS are almost constant, as the useful cooling effect, the electric and thermal power required are nearly not affected by ω_{out}, [6,30]. Only a very light increase of $COP_{El,sorpt}$ can be detected (Fig. 8b).

The contribution of the sorptive system to the overall cooling effect ($COP_{Th,sorpt}/COP_{Th}$) also slightly increases, from about 13% to about 16%.

To compensate for the lack of a climatic chamber in the test facility, which makes impossible to control inlet air temperature ($t_1 = t_{out}$) and humidity ratio ($\omega_1 = \omega_{out}$), experimental data showed in Figs. 4–6 have been taken from testing days where outlet temperature and humidity ratio were nearly constant, while experimental data of Figs. 7 and 8 were acquired during days with nearly constant values of the outlet humidity ratio (Fig. 7) or of the outlet temperature (Fig. 8). The same approach was also used in [6,30,34].

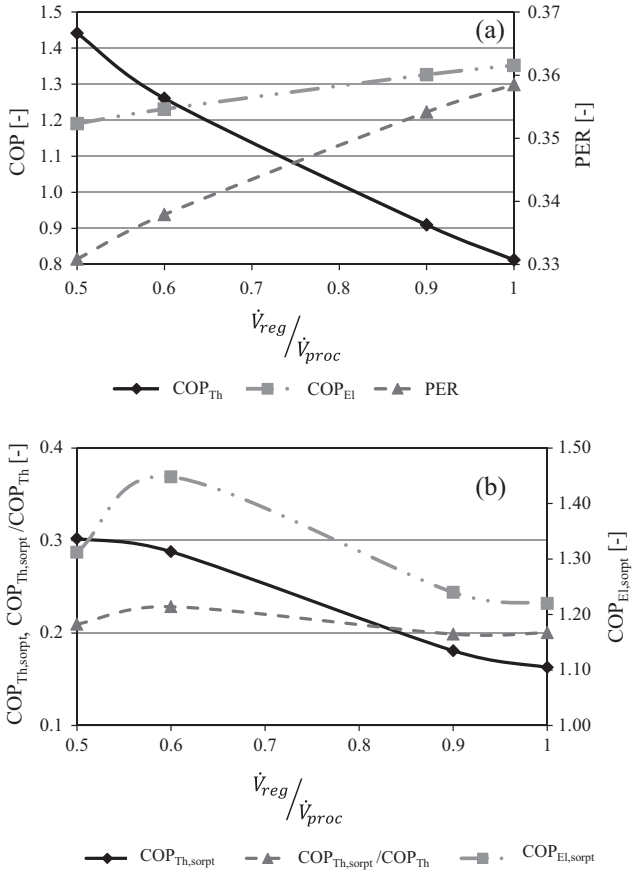

Fig. 6. Performance parameters as a function of ratio between regeneration and process air volumetric flow rate – t_{out} = 30.7 °C, ω_{out} = 7.83 g/kg, t_{reg} = 66.6 °C, N = 12 rev/h, t_{sup} = 14.4 °C, ω_{sup} = 3.24 g/kg, t_{w10} = 4.85 °C, COP^{VCS} = 2.13.

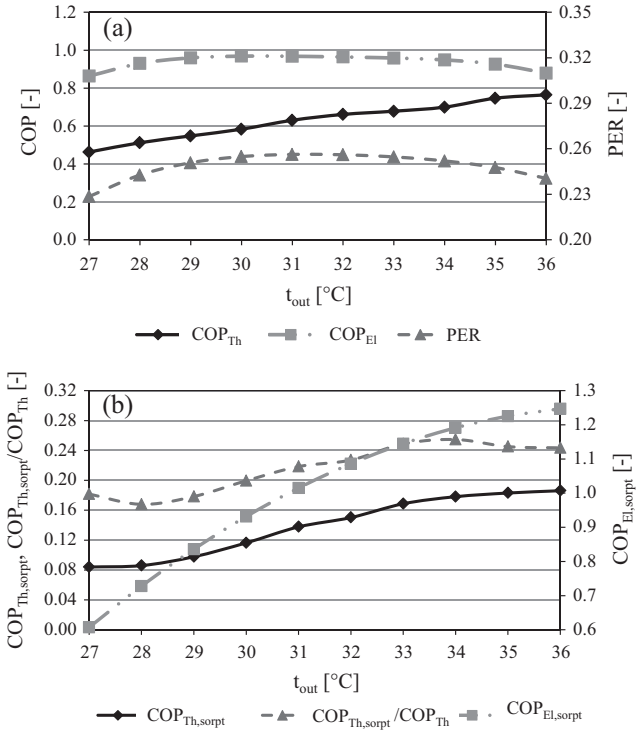

Fig. 7. Performance parameters as a function of outdoor air temperature – ω_{out} = 12.6 g/kg, t_{reg} = 65.0 °C, N = 12 rev/h, $\dot{V}_{proc}$ = 624 m^3/h, $\dot{V}_{reg}$ = 719 m^3/h, t_{sup} = 20.1 °C, ω_{sup} = 7.65 g/kg, t_{w10} = 11.3 °C, COP^{VCS} = 2.62.

4.2. Comparison between the hybrid DCS with MCHP and other air-conditioning options

4.2.1. Comparison with hybrid DCS with separate "production" systems

In this section the hybrid DCS with the MCHP (Fig. 1) is compared with the same DCS interacting with separate "production" (SP) systems: the electric grid for electricity supply and a natural gas boiler to provide regeneration thermal energy.

The PER of the DCS/SP system can be evaluated as:

$$PER^{DCS/SP} = \frac{NE_{Cool}^{DCS} + NE_{El}}{\frac{\left(NE_{El}+E_{El}^{aux}+E_{El}^{VCS}\right)}{\eta_{El,ref}} + \frac{\int \dot{m}_{reg}(h_8-h_1)d\tau}{\varepsilon_{hc}\cdot\eta_{Th,ref}}} \quad (10)$$

where NE_{El} (equal to NE_{El}^{MCHP}) is the net electricity provided to the final user (drawn by the electric grid), E_{El}^{aux} and E_{El}^{VCS} are electric energy consumption of the auxiliaries and the chiller, powered by the external grid too; regeneration thermal energy is fully provided by the natural gas boiler, through a heating coil with effectiveness ε_{hc} = 0.842, [27].

The comparison is performed in Fig. 9 where the *PER* of the DCS with MCHP and of the DCS with SP systems are shown as a function of t_{reg}. A maximum value of 65 °C is investigated (the boiler in the hybrid DCS with MCHP is not active). As seen, the increase of regeneration temperature determines a rise of the useful cooling effect (Fig. 4); however, the MCHP operates at constant conditions (full electric and thermal load), therefore its primary energy input does not change and the *PER* improves with t_{reg}; for the DCS with SP the increase of the cooling effect is offset by the related augmentation of the required regeneration thermal power, provided by the natural gas boiler.

For low values of t_{reg}, most part of thermal power from the MCHP is not used for regeneration and it is dissipated to the environment. The use of the microcogenerator is energetically feasible with respect to SP to feed the hybrid DCS when the regeneration temperature is higher than about 52 °C, which is the typical operating range of desiccant-based systems, as lower t_{reg} cannot achieve enough dehumidification capability, [6,30].

Similar conclusions can be drawn from the emissions analysis, as the $\Delta CO_{2,eq}$ becomes positive for regeneration temperatures higher than about 48 °C.

4.2.2. Comparison with hybrid DCS with separate "production" systems and integrated heat pump

One of the most efficient strategy to improve energy performance of hybrid DCS is the use of integrated heat pumps (HP), which consists of substituting the electric chiller with an electric heat pump integrated into the desiccant-based AHU. Cooling energy from the evaporator is used to balance the sensible load of the process air, while thermal energy from the condenser is used to pre-heat the regeneration air flow, [35,36].

In the existing configuration of the investigated test facility, the chiller provides only the cooling energy required to control the temperature of the supply process air, while dissipating in the environment thermal energy from the condenser. The current layout can be modified recovering part of the condensation thermal energy by drawing a share (800 m^3/h) of the air flow rate required by the condenser (3300 m^3/h) and carrying it in the regeneration air duct.

This modification is applied to the hybrid DCS with separate "production" systems described in Section 4.2.1, with the test conditions of Fig. 4. A part of the regeneration thermal power is

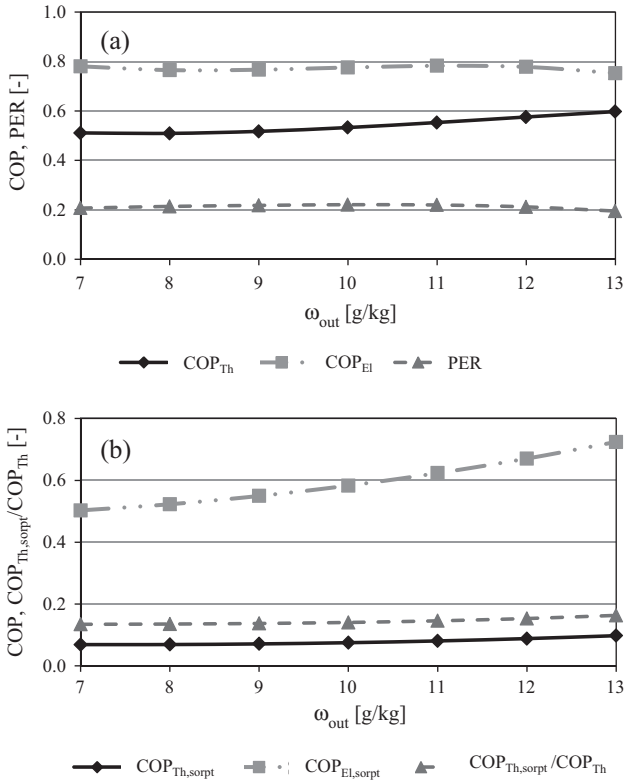

Fig. 8. performance parameters as a function of outdoor air humidity ratio – t_{out} = 32.7 °C, t_{reg} = 66.8 °C, N = 12 rev/h, $\dot{V}_{proc}$ = 575 m³/h, $\dot{V}_{reg}$ = 717 m³/h, t_{sup} = 17.2 °C (ω_{sup} is not specified, as it depends on ω_{out}), t_{w10} = 10.1 °C, COP^{VCS} = 2.35.

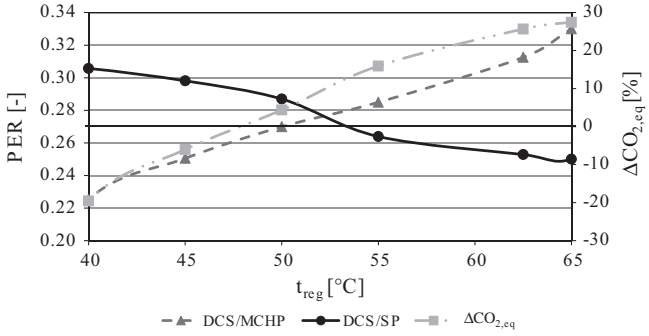

Fig. 9. Energy and environmental comparison between hybrid DCS with MCHP and with separate "production" (SP) systems – test conditions as in Fig. 4.

provided by the chiller condenser (the regeneration air stream is preheated by about 12–15 °C), and the remaining amount by the natural gas boiler. In this case, primary energy required by the boiler and the related $CO_{2,eq}$ emissions reduce. The results of the comparison with hybrid DCS with MCHP change from Figs. 9 and 10, which shows that the use of the microcogenerator is energetically feasible with respect to SP to feed the hybrid DCS when the regeneration temperature is higher than about 61 °C. The $\Delta CO_{2,eq}$ becomes positive for regeneration temperatures higher than about 55 °C.

A further comparison can be done with the system investigated by Beccali et al. [35]. A solar DCS, consisting of an AHU (process air flow rate 1250 m³/h) and flat plate collectors, was analyzed. A hybrid configuration was chosen, with two auxiliary cooling coils fed by a compression chiller, and which used the heat rejected by the chiller to preheat the regeneration airflow. Several efficiency

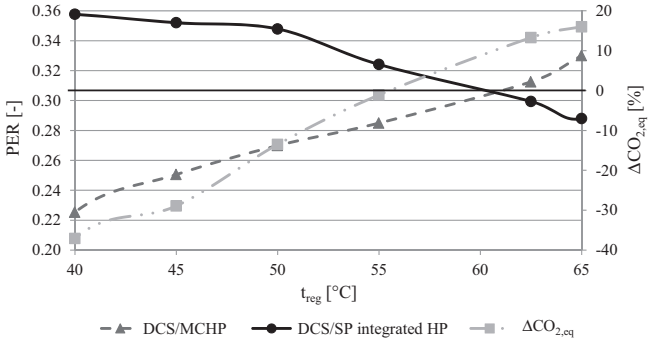

Fig. 10. Energy and environmental comparison between hybrid DCS with MCHP and with separate "production" (SP) systems and integrated HP – test conditions as in Fig. 4.

indicators were used to describe system performance, such as $COP_{Th,sorpt}$ and COP_{El}. The results of the monitoring were presented for a representative day in summer, with a maximum regeneration temperature of about 58 °C in the early afternoon. The corresponding outdoor air temperature and humidity ratio were about 30 °C and 14 g/kg, respectively. In the same time slot, $COP_{Th,sorpt}$ and COP_{El} ranged between 0.4–0.8 and 1.5–4, respectively. These values can be compared with those in Fig. 4a and b, which refers to very similar operating conditions. At the same t_{reg} = 58 °C, Fig. 4b provides $COP_{Th,sorpt}$ equal to about 0.2 and Fig. 4a shows COP_{El} equal to about 1.1, which are lower than the values achieved by the system investigated by Beccali et al. [35].

Therefore, the use of the condenser heat is a suitable approach to improve energy performance of hybrid DCS. A further advantage of this configuration is the contemporary between cooling power demand and heat rejection at the condenser. This strategy can also be applied when the DCS interacts with the MCHP, reducing thermal power provided by the cogenerator. However this option should be carefully investigated, as it could determine a reduction of the operating hours of the MCHP or partial load operation for the unit, with reduction of the total efficiency, unless the microcogenerator is forced to operate at full load by exploiting the thermal power not used for regeneration for other purposes (such as for domestic hot water demands).

4.2.3. Comparison with conventional AHU interacting with VCS

The comparison is performed between the hybrid DCS and a standard AHU, in which the process air is entirely drawn from outside (no recirculation is performed) and is dehumidified by means of a cooling coil connected to an electric VCS (process 1-A in Figs. 2 and 11), and is then post-heated by a natural gas boiler to the supply temperature (process A-5′ in Fig. 11), before being introduced in the conditioned space (state 5 in Figs. 2 and 11). State 5′ is not shown in Fig. 2 for major clarity, as it is very close to state 5. The standard AHU has the same inlet and supply conditions of the desiccant-based AHU.

The electric COP of this system is defined as:

$$COP_{El}^{AHU/VCS} = \frac{NE_{Cool}^{AHU/VCS}}{E_{El}^{AHU/VCS}} \tag{11}$$

where $NE_{Cool}^{AHU/VCS}$ is equal to the total cooling energy NE_{Cool}^{DCS} (Eq. (1)), as states 1 and 5 are the same for the DCS and for the AHU with VCS; $E_{El}^{AHU/VCS}$ is the overall electricity consumption of AHU/VCS: auxiliaries (one fan and two pumps, 0.62 kW total) and the electric chiller (E_{El}^{VCS}). The latter has been evaluated as:

$$E_{El}^{VCS} = \frac{\int \dot{m}_{proc} \cdot (h_1 - h_A) d\tau}{COP^{VCS}} \tag{12}$$

where COP^{VCS} is the COP of the electric chiller:

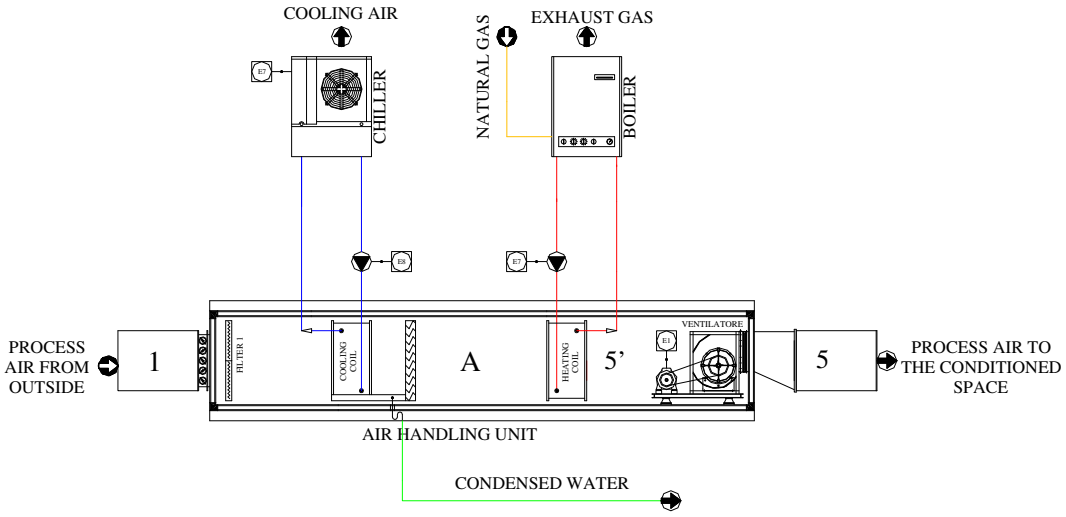

Fig. 11. Layout of the AHU with VCS.

$$COP^{VCS} = \frac{P_{Cool}^{VCS}}{P_{El}^{comp} + P_{El}^{fan}} \tag{13}$$

where P_{El}^{comp} and P_{El}^{fan} are the electric power required by the chiller compressor and by the condenser fan, respectively. COP^{VCS} is evaluated as a function of outdoor air temperature and supply air humidity ratio, by means of the data shown by Angrisani et al. [37].

State 'A' has been evaluated considering the by-pass factor:

$$F_{bp} = \frac{h_A - h_s}{h_1 - h_s} \tag{14}$$

where h_s is the enthalpy of humid air, in a saturated condition, at the surface temperature of the cooling coil (t_s). F_{bp} has been assumed equal to 0.177 [27], and t_s is evaluated by psychrometric calculations.

In Fig. 12, the electric COP values of the hybrid DCS and of the AHU/VCS are compared as a function of ω_{out}. The values of the corresponding ω_{sup} are also shown. COP^{VCS} strongly reduces for low values of ω_{sup}, as the VCS has to produce chilled water at very low temperatures to obtain the desired supply humidity ratio, [37], therefore COP_{El} of the AHU/VCS system decreases; the performance of the DCS system are instead almost insensitive to humidity ratio, [37], and it determines an electricity consumption reduction for ω_{out} less than about 9.5 g/kg.

As regards the comparison in terms of primary energy and equivalent CO_2 emissions savings of the hybrid DCS/MCHP system

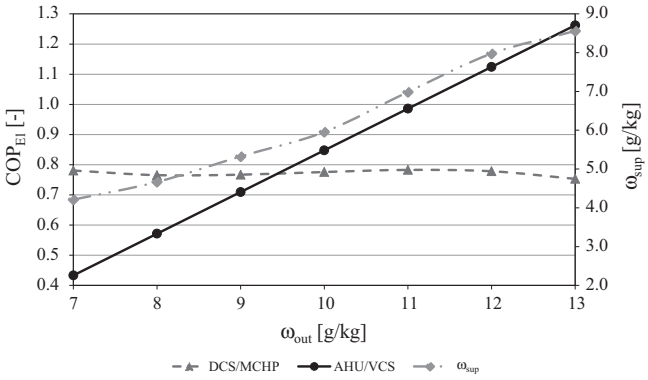

Fig. 12. Comparison between electric COP of DCS/MCHP system and AHU/VCS as a function of outdoor air humidity ratio – test conditions as in Fig. 8.

with respect to the AHU/VCS, the analysis was performed in a previous work, [37]. Results stated that the desiccant-based AHU interacting with the microcogenerator can guarantee primary energy and emissions saving when outdoor air humidity ratio is lower than a certain value, and that energy and environmental benefits increase with outdoor air temperature.

4.2.4. Comparison with conventional AHU interacting with absorption chiller

Absorption refrigeration is the most widely used thermally-activated cooling system, [38]. Substitution of the compressor of VCS with a thermally driven mechanism is the main difference of the absorption refrigeration cycle, which requires very low electric input. Usually its components are an absorber, a pump, an expansion valve, a generator, a regenerator, a condenser and an evaporator. The working fluid is a solution of a sorbent and a refrigerant: water–ammonia (H_2O–NH_3) or lithium bromide–water (LiBr–H_2O) are typically used. The refrigerant provides the useful cooling effect in the evaporator, while thermal energy from the condenser and from the absorber is rejected to the ambient. Thermal energy is required in the generator to separate the sorbent which has absorbed the refrigerant in the absorber.

Considering the maximum value of regeneration temperature achievable in the test facility investigated in this paper (70 °C, see Fig. 4), a half effect H_2O–LiBr system could be driven. The half effect cycle includes two solution circuits, [39]. Both of them include a generator and an absorber. The vapor generated in the generator of the low pressure circuit enters in the absorber of the high pressure circuit. Heat is supplied at the same temperature to both generators and dissipated at an intermediate temperature in the condenser and in the low and high pressure absorbers. This configuration can work at a considerably lower generator temperature than the single-effect cycle, but at the cost of a lower COP.

The hybrid DCS investigated in this paper is compared with the absorption cycle, considering for the latter the same conventional AHU layout of Fig. 11, substituting the electric chiller with a half effect H_2O–LiBr absorption chiller (ACH). The thermal COP of the overall system is defined as:

$$COP_{Th}^{AHU/ACH} = \frac{NE_{Cool}^{AHU/ACH}}{E_{Th}^{AHU/ACH}} \tag{15}$$

where $NE_{Cool}^{AHU/ACH}$ is equal to NE_{Cool}^{DCS} (Eq. (1)), as states 1 and 5 are the same for DCS and for the AHU with ACH; $E_{Th}^{AHU/ACH}$ is the sum of

thermal energy consumption for air post heating (E_{Th}^{ph}) and to drive the ACH (E_{Th}^{ACH}).

$$E_{Th}^{ph} = \frac{\int \dot{m}_{proc} \cdot (h_A - h_{5'}) d\tau}{\varepsilon_{hc}} \quad (16)$$

where ε_{hc} is the effectiveness of the heating coil (0.842, [27]).

$$E_{Th}^{ACH} = \frac{\int \dot{m}_{proc} \cdot (h_1 - h_A) d\tau}{COP^{ACH}} \quad (17)$$

Ferreira and Kin [40] reported typical COP values of absorption cycles. For a H_2O–LiBr half effect absorption system, with regeneration temperature of 67 °C and ambient rejection temperature of 30 °C, a COP^{ACH} of 0.35 is indicated.

Considering the operating conditions of Fig. 7, with t_{out} = 30 °C, a $COP_{Th}^{AHU/ACH}$ equal to 0.279 would be obtained, which is lower than COP_{Th} of the DCS from Fig. 6a, which is about 0.6 for an outdoor air temperature of 30 °C.

The *PER* of the AHU/ACH system at t_{out} = 30 °C can be evaluated, similarly to Eq. (10), as:

$$PER^{AHU/ACH} = \frac{NE_{Cool}^{AHU/ACH} + NE_{El}}{\frac{\left(NE_{El} + E_{El}^{aux}\right)}{\eta_{El,ref}} + \frac{E_{Th}^{ACH} + E_{Th}^{ph}}{\varepsilon_{hc} \cdot \eta_{Th,ref}}} = 0.173 \quad (18)$$

which is lower than the corresponding value for the DCS/MCHP system for all values of t_{out} (see Fig. 7a).

The corresponding $\Delta CO_{2,eq}$ would be about 34% at t_{out} = 30 °C.

As regards the performance of the single components (DW and ACH), Kalkan et al. [41] showed thermal COP of absorption chillers as a function of heat supply temperature; it ranges from about 0.2 for t_{reg} = 60 °C to about 0.6 for t_{reg} = 70 °C. The corresponding values of $COP_{Th,sorpt}$ for the DCS are lower: from about 0.2 for t_{reg} = 60 °C to about 0.18 for t_{reg} = 70 °C (Fig. 4b). Nevertheless, as shown, thermal and primary energy-based performance of the overall hybrid DCS/MCHP system are higher than those of the AHU/ACH system, with also minor equivalent CO_2 emissions.

4.2.5. Comparison with conventional AHU interacting with adsorption chiller

Adsorption chiller are based on the same operating principle as desiccant wheels: adsorbents like zeolite, silica gel, activated carbon and alumina have highly porous structures with surface–volume ratios in the order of several hundreds that can selectively catch and hold refrigerants. When saturated, they can be regenerated by being heated. If an adsorbent and a refrigerant are contained in the same vessel, the adsorbent would adsorb the evaporating refrigerant. The process is intermittent because the adsorbent must be regenerated when it is saturated. For this reason, multiple adsorbent beds are required for continuous operation, [40].

Adsorption chillers using silica gel–water working pairs have been commercialized, because such cooling systems can be powered with 60–90 °C hot water directly and can be effectively used in trigeneration systems, with thermal COP in the range 0.30–0.40, [42–44].

Kong et al. [45] described an experimental investigation of the performance of a small scale trigeneration system, with an adsorption chiller (ADCH) with a rated cooling capacity of 9 kW. Silica gel–water was used as working pair in the adsorption cooling system. Results showed that the COP of the adsorption chiller with hot water inlet temperature of 65 °C, chilled water inlet temperature of 15.7 °C and cooling water inlet temperature of 30.7 °C is about 0.3.

The comparison with the hybrid DCS/MCHP is performed considering the same layout of Fig. 11, substituting the electric VCS with the ADCH, and applying Eqs. (15)–(17) to calculate $COP_{Th}^{AHU/ADCH}$. By applying COP^{ADCH} = 0.3, a $COP_{Th}^{AHU/ADCH}$ equal to 0.245 was obtained, which is lower than COP_{Th} of the DCS from Fig. 7a in the whole range of outdoor air temperature.

A further comparison can be performed considering that the most recent improvements in adsorption chillers provided a thermal COP of 0.55 with 65 °C thermal waste, [42]. Even using this higher COP^{ADCH}, the overall performance factor is $COP_{Th}^{AHU/ADCH}$ = 0.424 (at t_{out} = 30.7 °C), which continues to be lower than COP_{Th} of the DCS from Fig. 7a in the whole range of outdoor air temperature. A further improvement of 9% of the thermal COP of ADCH is expected in next years, [43].

The PER of the overall AHU/ADCH, considering COP^{ADCH} = 0.55 and applying Eqs. (17) and (18), is about 0.248 (at t_{out} = 30.7 °C), which confirms better performance of the DCS/MCHP system. In the same conditions, the reduction of equivalent CO_2 emissions would be about 8.6%.

Also in this case, thermal performance of the single component (ADCH) are better than those of the desiccant rotor; COP^{ADCH} ranges from 0.30 to 0.33, when heat source temperature increases from 60 to 70 °C, [45]; correspondingly, $COP_{Th,sorpt}$ for the DCS is slightly lower: from about 0.2 for t_{reg} = 60 °C to about 0.18 for t_{reg} = 70 °C (Fig. 4b).

4.2.6. Comparison with liquid desiccant air-conditioning system

As an alternative to solid DCS, liquid desiccant air-conditioning (LDAC) systems have developed quickly in recent years. The driving force of moisture removal by the liquid desiccant is the water vapor pressure difference between the desiccant solution and the air. The moisture in air is absorbed by the strong desiccant solution, while the sensible load can be removed by cooling device with relatively high temperature water, [46,47]. The desiccant solution can be regenerated at temperatures as low as 65–80 °C, which allow to match LDAC systems with renewable energy-based technologies too, [48–50].

Research activities have been performed at Tsinghua University in this regard [51]; the authors evaluated the performance of a heat-driven LDAC system with the summer outdoor climate in Beijing, with a regeneration temperature of 75 °C. Considering the outdoor conditions of Fig. 5 (t_{out} = 34.1 °C, ω_{out} = 11.6 g/kg), the resulting thermal COP of the LDAC is about 1.5, which is lower than the COP_{Th} of the investigated solid DCS in the whole range of rotational speed of the desiccant wheel (see Fig. 5a).

A further comparison can be done with the experimental results shown by Crofoot and Harrison [52], in the Queen's University Solar Liquid Desiccant Cooling Demonstration project, aimed to evaluate the feasibility of a solar LDAC in Canada and other temperate climates. The LDAC is a prototype commercially available desiccant system designed for building applications. The solar LDAC has been operated and monitored between 8 am and 6 pm for five days in June and July 2012. In particular the conditions of 29 June 2012 (average ambient temperature 27.6 °C, average ambient humidity 12.2 g/kg, average process air supply humidity 8.1 g/kg) are very similar to those of Fig. 7 (average ambient humidity 12.6 g/kg, average process air supply humidity ratio 7.65 g/kg); Fig. 7a with t_{out} = 27.6 °C provides a COP_{Th} of about 0.50, which is comparable with the value 0.49 given by Crofoot and Harrison [52] for the LDAC.

The data in Fig. 7a can be also compared with the results shown by Scalabrin and Scaltriti [53], where an open process of summer air-conditioning by dehumidification was presented and simulated. Air dehumidification was achieved in an absorption column through direct contact with a hygroscopic solution over a cooling tube bank inside which water flowed, coming from a cooling tower. The diluted solution was reconcentrated in a desorber by direct contact with external air over a heating tube bank, inside which water flowed, coming from an external heating or heat recovery system. The system was tested considering outdoor

Table 2
Specific investment cost for the different air-conditioning systems.

	DCS with VCS	Conventional AHU with VCS	Conventional AHU with ACH	Conventional AHU with ADCH	LDAC with VCS
Cost of AHU (€/kW)	1390 [55]	300 [56]	300 [56]	300 [56]	500–600 [42,57]
Cost of cooling device (€/kW)	400 [10]	400 [10]	700 [40]	1000–2000 [42]	400 [10]
Total cost (€/kW)	1790	700	1000	1300–2300	900–1000

condition of 34 °C and 13 g/kg, room condition of 26 °C and 12.6 g/kg, providing a thermal COP of 0.70. This value is very similar to that of Fig. 7a, however the quite high COP of the investigated LDAC can be attributed to very low moisture difference between outdoor and room air, [54].

For the LDAC system, the analysis based on *PER* and $\Delta CO_{2,eq}$ cannot be performed, as no data about electric consumption of the air-conditioning systems are available.

4.2.7. Concluding remarks

As seen from the previous sections, hybrid DCS can have better energy and emissions performance with respect to other thermally activated cooling technologies. DCS systems are also very reliable and easy for maintenance, while they have the problem of the quite big size of the AHU, due to the space required by the desiccant wheel cassette.

In terms of economic analysis, as desiccant cooling systems are heat driven components, they are effective for air-conditioning in residential buildings in regions where the use of thermal energy is more economical than electrical power, or when "free" thermal energy is available, i.e. coming from solar collectors or thermal wastes. As regards the initial cost, the specific investment cost for the different air-conditioning systems investigated in this paper is shown in Table 2, considering the prices of the AHU and of the cooling device. For the LDAC, it was assumed that the sensible load is balanced by a VCS. The DCS with VCS is one of the most expensive technology, therefore a reduction of the installation cost is strictly required, to benefit from the energy and environmental advantages of desiccant cooling.

5. Conclusions

In this work, a hybrid desiccant cooling system (DCS) with a silica gel desiccant rotor, interacting with a small scale cogenerator, is experimentally analyzed. The microcogenerator provides electric energy for the auxiliaries and for the chiller which contributes to balance the sensible cooling load; regeneration energy is provided by thermal wastes of the cogenerator and by a natural gas boiler.

Both the overall DCS and the adsorbent rotor alone were considered; the effect on performance of five operating conditions is analyzed: regeneration temperature, rotational speed, ratio between flow rates of regeneration to process air, outdoor air temperature and humidity ratio. Several performance parameters, based on electric, thermal and primary energy, are used.

Results show that thermal performance reduce when regeneration temperature or regeneration flow rate increases, while electric and primary energy based parameters rise, thanks to the increase of the useful cooling effect provided by the DCS. Furthermore, optimal operation is found for a narrow range of rotational speed (about 2–7.5 rev/h), while outdoor air temperature and humidity ratio have a very weak effect.

The sorptive part of the hybrid desiccant cooling system provided a limited amount of the overall cooling effect (in the range 15–35%); however, the desiccant dehumidification process allows to operate the electric chiller with a higher chilled water temperature, increasing the performance of the chiller itself and of the overall system.

The hybrid desiccant cooling system is then compared, in terms of both energy and equivalent CO_2 emissions, with other air-conditioning technologies: hybrid DCS with "separate" production systems (with and without integrated heat pump), liquid desiccant cooling as well as conventional air handling unit interacting with electric vapor compression, absorption or adsorption chiller. The performance of the investigated hybrid DCS with microcogenerator are higher or at least equal than those of the other thermally-activated technologies, with emissions reductions up to 34%; the result of the comparison with the conventional electric unit depends on outdoor air conditions, which strongly affect the COP of the vapor compression device.

The recovery of the condenser heat is a suitable approach to improve energy performance of hybrid DCS, mainly when it is supplied by separate "production" systems.

In conclusion, hybrid desiccant cooling systems have a high potential to be energetically competitive and environmentally friendly with respect to other thermally activated cooling technologies in all operating conditions. In particular, the performance of the investigated DCS/MCHP system improve when either the temperature or the volumetric flow rate of the regeneration air increases, when very low values of supply air humidity ratio are required, such as in high latent load applications, or when outdoor process air temperature rises.

The comparison with the conventional electric units is still unfavourable in certain climatic conditions, such as high humidity ratio of inlet process air, therefore there is the need to improve thermal and electric COP of desiccant cooling system.

Furthermore, hybrid DCS are currently an expensive technology, therefore a reduction of the investment cost is desirable, to exploit its energy and environmental advantages.

References

[1] Ruivo CR, Angrisani G. The effectiveness method to predict the behaviour of a desiccant wheel: an attempt of experimental validation. Appl Therm Eng. 2014;71:643–51.
[2] Henning HM, Pagano T, Mola S, Wiemken E. Micro tri-generation system for indoor air conditioning in the Mediterranean climate. Appl Therm Eng 2007;27:2188–94.
[3] Capozzoli A, Mazzei P, Minichiello F, Palma D. Hybrid HVAC systems with chemical dehumidification for supermarket applications. Appl Therm Eng 2006;26:795–805.
[4] Xiao F, Ge G, Niu X. Control performance of a dedicated outdoor air system adopting liquid desiccant dehumidification. Appl Energy 2011;88:143–9.
[5] Ge G, Xiao F, Xu X. Model-based optimal control of a dedicated outdoor air-chilled ceiling system using liquid desiccant and membrane-based total heat recovery. Appl Energy 2011;88:4180–90.
[6] Angrisani G, Capozzoli A, Minichiello F, Roselli C, Sasso M. Desiccant wheel regenerated by thermal energy from a microcogenerator: experimental assessment of the performances. Appl Energy 2011;88:1354–65.
[7] Calise F, Dentice d'Accadia M, Roselli C, Sasso M, Tariello F. Desiccant-based AHU interacting with a CPVT collector: simulation of energy and environmental performance. Sol Energy 2013, <http://dx.doi.org/10.1016/j.solener.2013.11.001> [in press].
[8] Wang X, Cai W, Lu J, Sun Y, Ding X. A hybrid dehumidifier model for real-time performance monitoring, control and optimization in liquid desiccant dehumidification system. Appl Energy 2013;111:449–55.
[9] Qi R, Lu L, Yang H, Qin F. Investigation on wetted area and film thickness for falling film liquid desiccant regeneration system. Appl Energy 2013;112:93–101.
[10] Angrisani G, Roselli C, Sasso M, Tariello F. Dynamic performance assessment of a micro-trigeneration system with a desiccant-based air handling unit in Southern Italy climatic conditions. Energy Convers Manage 2014;80:188–201.

[11] Ge TS, Dai YJ, Li Y, Wang RZ. Simulation investigation on solar powered desiccant coated heat exchanger cooling system. Appl Energy 2012;93:532–40.
[12] Gonçalves P, Angrisani G, Sasso M, Rodrigues Gaspar A, Gameiro da Silva M. Exergetic analysis of a desiccant cooling system: searching for performance improvement opportunities. Int J Energy Res 2014;38:714–27.
[13] Xiong ZQ, Dai YJ, Wang RZ. Development of a novel two-stage liquid desiccant dehumidification system assisted by CaCl2 solution using exergy analysis method. Appl Energy 2010;87:1495–504.
[14] Panaras G, Mathioulakis E, Belessiotis V. Solid desiccant air-conditioning systems – design parameters. Energy 2011;36:2399–406.
[15] Heidarinejad G, Pasdarshahri H. The effects of operational conditions of the desiccant wheel on the performance of desiccant cooling cycles. Energy Build 2010;42:2416–23.
[16] Heidarinejad G, Pasdarshahri H. Potential of a desiccant-evaporative cooling system performance in a multi-climate country. Int J Refrig 2011;34:1251–61.
[17] Nóbrega CEL, Brum NCL. A graphical procedure for desiccant cooling cycle design. Energy 2011;36:1564–70.
[18] Jalalzadeh-Azar A, Slayzak S, Judkoff R, Schaffhauser T, DeBlasio R. Performance assessment of a desiccant cooling system in a CHP application incorporating an IC engine. Int J Distrib Energy Resour 2005;1:163–84.
[19] Hürdoğan E, Büyükalaca O, Yılmaz T, Hepbaşlı A. Experimental investigation of a novel desiccant cooling system. Energy Build 2010;42:2049–60.
[20] Ali Mandegari M, Pahlavanzadeh H. Performance assessment of hybrid desiccant cooling system at various climates. Energy Efficiency 2010;3:177–87.
[21] Çarpinlioglu MÖ, Yildirim M. A methodology for the performance evaluation of an experimental desiccant cooling system. Int Commun Heat Mass Trans 2005;32:1400–10.
[22] Eicker U, Schürger U, Köhler M, Ge T, Dai YJ, Li H, et al. Experimental investigations on desiccant wheels. Appl Therm Eng 2012;42:71–80.
[23] Tu R, Liu XH, Jiang Y. Performance analysis of a two-stage desiccant cooling system. Appl Energy 2014;113:1562–74.
[24] Griffiths B. Optimizing the energy efficiency of desiccant dehumidifiers. HPAC Eng December 2011. <http://hpac.com/humidification-dehumidification/optimizing-desiccant-dehumidifiers-1211/> [accessed 04.07.14].
[25] Ruivo CR, Carrillo-Andrés A, Costa JJ, Domínguez-Muñoz F. Exponential correlations to predict the dependence of effectiveness parameters of a desiccant wheel on the airflow rates and on the rotation speed. Appl Therm Eng 2013;51:442–50.
[26] Angrisani G, Roselli C, Sasso M. Effect of rotational speed on the performances of a desiccant wheel. Appl Energy 2013;104:268–75.
[27] Angrisani G, Roselli C, Sasso M. Experimental validation of constant efficiency models for the subsystems of an unconventional desiccant-based air handling unit and investigation of its performance. Appl Therm Eng 2012;33–34:100–8.
[28] Jia CX, Dai YJ, Wu JY, Wang RZ. Use of compound desiccant to develop high performance desiccant cooling system. Int J Refrig 2007;30:345–53.
[29] Sibilio S, Sasso M, Possidente R, Roselli C. Assessment of micro-cogeneration potential for domestic trigeneration. Int J Environ Technol Manage 2007;7:147–64.
[30] Angrisani G, Minichiello F, Roselli C, Sasso M. Experimental analysis on the dehumidification and thermal performance of a desiccant wheel. Appl Energy 2012;92:563–72.
[31] Ge TS, Ziegler F, Wang RZ, Wang H. Performance comparison between a solar driven rotary desiccant cooling system and conventional vapor compression system (performance study of desiccant cooling). Appl Therm Eng 2010;30:724–31.
[32] Wang RZ, Ge TS, Chen CJ, Ma Q, Xiong ZQ. Solar sorption cooling systems for residential applications: options and guidelines. Int J Refrig 2009;32:638–60.
[33] Ge TS, Li Y, Wang RZ, Dai YJ. Experimental study on a two-stage rotary desiccant cooling system. Int J Refrig 2009;32:498–508.
[34] Angrisani G, Minichiello F, Roselli C, Sasso M. Desiccant HVAC system driven by a micro-CHP: experimental analysis. Energy Build 2010;42:2028–35.
[35] Beccali M, Finocchiaro P, Noche B. Energy performance evaluation of a demo solar desiccant cooling system with heat recovery for the regeneration of the adsorption material. Renew Energy 2012;44:40–52.
[36] Sukamongkol Y, Chungpaibulpatana S, Limmeechokchai B, Sripadungtham P. Condenser heat recovery with a PV/T air heating collector to regenerate desiccant for reducing energy use of an air conditioning room. Energy Build 2010;42:315–25.
[37] Angrisani G, Minichiello F, Roselli C, Sasso M. Experimental investigation to optimise a desiccant HVAC system coupled to a small size cogenerator. Appl Therm Eng 2011;31:506–12.
[38] International Energy Agency. Ongoing research relevant for solid assisted air conditioning systems technical report. IEA Solar Heating and Cooling Task 25: Solar-assisted Air-conditioning of Buildings; 2002.
[39] Gebreslassie BH, Medrano M, Boer D. Exergy analysis of multi-effect water–LiBr absorption systems: from half to triple effect. Renew Energy 2010;35:1773–82.
[40] Ferreira CI, Kim DS. Techno-economic review of solar cooling technologies based on location-specific data. Int J Refrig 2014;39:23–37.
[41] Kalkan N, Young EA, Celiktas A. Solar thermal air conditioning technology reducing the footprint of solar thermal air conditioning. Renew Sustain Energy Rev 2012;16:6352–83.
[42] Deng J, Wang RZ, Han GY. A review of thermally activated cooling technologies for combined cooling, heating and power systems. Prog Energy Combust Sci 2011;37:172–203.
[43] Schall D, Hirzel S. Thermal cooling using low-temperature waste heat: a cost-effective way for industrial companies to improve energy efficiency? Energy Efficiency 2012;5:547–69.
[44] Zhai XQ, Wang RZ. A review for absorbtion and adsorption solar cooling systems in China. Renew Sustain Energy Rev 2009;13:1523–31.
[45] Kong XQ, Wang RZ, Wu JY, Huang XH, Huangfu Y, Wu DW, et al. Experimental investigation of a micro-combined cooling, heating and power system driven by a gas engine. Int J Refrig 2005;28:977–87.
[46] Niu X, Xiao F, Ge G. Performance analysis of liquid desiccant based air-conditioning system under variable fresh air ratios. Energy Build 2010;42:2457–64.
[47] Abdel-Salam AH, Simonson CJ. Annual evaluation of energy, environmental and economic performances of a membrane liquid desiccant air conditioning system with/without ERV. Appl Energy 2014;116:134–48.
[48] Li XW, Zhang XS, Quan S. Single-stage and double-stage photovoltaic driven regeneration for liquid desiccant cooling system. Appl Energy 2011;88:4908–17.
[49] Audah N, Ghaddar N, Ghali K. Optimized solar-powered liquid desiccant system to supply building fresh water and cooling needs. Appl Energy 2011;88:3726–36.
[50] Peng D, Zhang X. An analytical model for coupled heat and mass transfer processes in solar collector/regenerator using liquid desiccant. Appl Energy 2011;88:2436–44.
[51] Liu X, Jiang Y, Liu S, Chen X. Research progress in liquid desiccant air-conditioning devices and systems. Front Energy Power Eng China 2010;4:55–65.
[52] Crofoot L, Harrison S. Performance evaluation of a liquid desiccant solar air conditioning system. Energy Procedia 2012;30:542–50.
[53] Scalabrin G, Scaltriti G. A liquid sorption-desorption system for air conditioning with heat at lower temperature. ASME J Sol Energy Eng 1990;112:70–5.
[54] Kumar R, Dhar PL, Jain S, Asati AK. Multi absorber stand alone liquid desiccant air-conditioning systems for higher performance. Sol Energy 2009;83:761–72.
[55] <http://www.roccheggiani.it/online/home.php?language=en>; [accessed 21.07.14].
[56] <http://www.sabiana.it/en/home.php>; [accessed 21.07.14].
[57] Badami M, Portoraro A. Performance analysis of an innovative small-scale trigeneration plant with liquid desiccant cooling system. Energy Build 2009;41:1195–204.